Anisotropy of acousto-optic figure of merit in the *XZ* plane of $Pb_5Ge_3O_{11}$ crystals

Mys O., Orykhivskyi I., Kostyrko M. and Vlokh R.

O. G. Vlokh Institute of Physical Optics, 23 Dragomanov Street, 79005 Lviv, Ukraine

Received: 30.03.2021

Abstract. We use both numerical and analytical approaches when deriving phenomenological relations for the effective elasto-optic coefficients. Anisotropies of the effective elasto-optic coefficients and the acousto-optic (AO) figure of merit are calculated for a particular case of AO interactions in the principal *XZ* plane of $Pb_5Ge_3O_{11}$ crystals. Using the approximation of linearly polarized optical eigenwaves, we find that the maximal AO figure of merit for the isotropic diffraction is equal to 30.3×10^{-15} s^3/kg. It is achieved for the AO interactions of the type II at the angle $\theta = 10$ deg with respect to the *X* axis. In case of the anisotropic AO diffraction, the appropriate maximum, 12.4×10^{-15} s^3/kg, is reached for the AO interactions of the type IX at the angle $\theta = 187.9$ deg.

Keywords: acousto-optics, anisotropy, lead germanate crystals

UDC: 535.4+535.55

1. Introduction

Lead germanate crystals, $Pb_5Ge_3O_{11}$, is a canonical ferroelectric material that undergos a proper ferroelectric phase transition at 450 K with the symmetry change $\bar{6} \Leftrightarrow 3$ [1]. The attenuation of acoustic waves (AWs) in these crystals in the gigahertz frequency range is high enough [2], thus making lead germanate unsuitable for any acousto-optic (AO) applications. However, the attenuation of AWs falls down to ~ 1 dB/cm in the megahertz range. This leaves a possibility for wide applications of $Pb_5Ge_3O_{11}$ as a working material for various AO devices.

It is known that lead germanate is optically active. The optical rotation occurring under light propagation along the polar axis is equal to ±5.58 deg/mm [3], while switching of the spontaneous polarization leads to changing optical activity sign, since the ferroelectric domains are enantiomorphous. This phenomenon is also interesting from the viewpoint of quantum optics when the AO interactions between circularly polarized optical eigenwaves and AWs are considered. Recently we have shown that the interactions of circularly polarized optical eigenwaves can be considered as a separate type of AO interactions [4−6], which is analogous to the interactions between linearly polarized optical eigenwaves. Nevertheless, the anisotropy of the main AO parameter, AO figure of merit, has not yet been studied for the lead germanate crystals, even in the simplest case of interactions between the linearly polarized optical waves and the AWs.

It is well known that the AO figure of merit is determined by the relation

$$M_2 = \frac{n_o^3 n_e^3 p_{eff}^2}{\rho v_{ij}^3}, \tag{1}$$

where $n_o = 2.116$ and $n_e = 2.151$ are respectively the ordinary and extraordinary refractive indices [1], p_{eff} denotes the effective elasto-optic coefficient (EEC), v_{ij} the AW velocity (with the

subscript *i* defining the propagation direction of AW and *j* giving the direction of its polarization), and $\rho = 7.33\times10^3$ kg/m^3 the density of material [7]. The M_2 parameter is responsible for the efficiency of AO diffraction. Note that the matrices of elasto-optic and elastic-stiffness coefficients are far from being sparse for the case of point symmetry group 3 peculiar for $Pb_5Ge_3O_{11}$ [8]. In other words, these crystals manifest relatively low symmetry, in spite of the fact that $Pb_5Ge_3O_{11}$ is an optically uniaxial material. Moreover, this property gives rise to a complicated non-orthogonality of AW polarizations, which manifests itself in a rotation of displacement vector around the three principal axes [6, 9], as a result of cumbersome analytical relations for the EECs. Furthermore, only three planes containing a three-fold symmetry axis are available in the crystals of the symmetry group 3, such that the displacement vector and the AW wave vector both lie in these planes. The above planes are formed from so-called second-kind directions [10–12]. Two of the acoustic eigenwaves propagating along these directions are non-orthogonal. These are a quasi-longitudinal (QL) AW and a quasi-transverse (QT) AW. The third acoustic eigenwave is purely transverse (PT). One of these special planes in lead germanate coincides with the *XZ* plane, while the other two are rotated by ±120 deg around the *Z* axis with respect to the *XZ* plane.

For the AWs propagating in these planes, the Christoffel tensor M_{kl} contains a single off-diagonal component. Hence, the angle of non-orthogonality ζ_m can be obtained analytically:

$$\tan 2\zeta_2 = \frac{2M_{13}}{M_{11} - M_{33}}. \tag{2}$$

As a consequence, the projections of the mechanical displacement vector on the coordinate axes and the mechanical strain tensor components can also be derived analytically. Using known strain tensor components, one can obtain the analytical relations for the EECs [13]. Otherwise, one has to employ a numerical approach for obtaining the eigenvectors of acoustic eigenwaves, and the strain tensor components can be obtained via coordinate differentiation.

In the present work, we use both the analytical and numerical approaches and verify their agreement, taking $Pb_5Ge_3O_{11}$ crystals as an example. These approaches are applied for the three interaction planes containing the second-kind directions. Finally, the relations for the EECs are obtained and the anisotropy of AO figure of merit is analyzed for the AW propagation directions lying in the above planes. Note that we neglect any manifestations of the optical activity effect in our analysis, though analyze the relevant implications.

2. Methods of analysis

2.1. Isotropic AO interactions

We start with deriving the EEC. Let us begin with consideration of the method based on the projections of displacement vector upon the directions of the wave vector and its perpendicular. Let the QL AW propagate in the *XZ* plane at the angle θ with respect to the *X* axis, while the displacement vector of this AW lie at the angle ζ_2 with respect to the *X* axis. The longitudinal (u_L) and transverse (u_T) components of the unit displacement vector (see Fig. 1) can be written as a projection of the vector *u* on the X' and Z' axes, respectively:

$$\begin{aligned} u_L &= u\cos(\zeta_2 - \theta)\cos(\Omega t - K_{X'}X'), \\ u_T &= u\sin(\zeta_2 - \theta)\cos(\Omega t - K_{X'}X') \end{aligned}, \tag{1}$$

where $K_{X'}$ denotes the AW wave vector, Ω the AW frequency, and *t* time. The strain tensor components in the coordinate system $X'Z'$ are written as partial derivatives of the displacement components with respect to coordinates:

$$e_1' = \frac{\partial u_L}{\partial X'} = uK_{X'}\cos(\zeta_2 - \theta)\sin(\Omega t - K_{X'}X'),$$
$$e_5' = 2e_{13}' = \frac{\partial u_L}{\partial Z'} + \frac{\partial u_T}{\partial X'} = uK_{X'}\sin(\zeta_2 - \theta)\sin(\Omega t - K_{X'}X'). \quad (2)$$

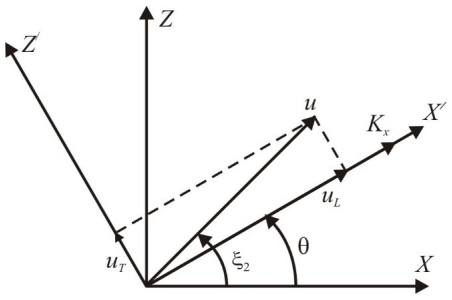

Fig. 1. Schematic view of AW propagation in the *XZ* and $X'Z'$ coordinate systems of lead germanate.

Here $\boldsymbol{K}_{X'}$ is accepted to be the unit vector. In the coordinate system *XZ*, the amplitudes of the strain components read as

$$e_1 = \cos\theta\cos\zeta_2,$$
$$e_3 = \sin\theta\sin\zeta_2, \quad (3)$$
$$e_5 = \sin(\zeta_2 + \theta).$$

If the incident and diffracted optical waves propagate in the *XZ* plane and are polarized parallel to the *Y* axis, the electric field of the diffracted wave is given by

$$E_2 = \Delta B_{22} D_2 \cos\left[(\omega \pm \Omega)t - (k_i \pm K_{X'})X'\right], \quad (4)$$

where D_2 denotes the unit amplitude of the electric displacement component of the incident optical wave, k_i the wave vector of the incident optical wave, and ω the incident optical-wave frequency. Then the intensity of the diffractive optical wave *I* is proportional to the square of its electric field component. With accounting for the relation $\left\langle \cos^2((\omega \pm \Omega)t - (k_i \pm K_{X'})X')\right\rangle = 1/2$ we arrive at

$$I \propto E_2^2 = \Delta B_{22}^2 \cos^2\left[(\omega \pm \Omega)t - (k_i \pm K_{X'})X'\right] = 0.5\Delta B_{22}^2. \quad (5)$$

Finally, the squared EEC for the type I of AO interactions is equal to

$$p_{eff}^{2(I)} = 0.5(p_{12}e_1 + p_{23}e_3 + p_{25}e_5)^2. \quad (6)$$

When the incident and diffracted optical waves are polarized in the *XZ* plane, the electric field of the diffracted optical wave is determined by the system

$$\begin{cases} E_1 = \Delta B_{11} D_1 + \Delta B_{13} D_3 \\ E_3 = \Delta B_{13} D_1 + \Delta B_{33} D_3 \end{cases},$$
$$\begin{cases} E_1 = \left(\Delta B_{11}\cos(\theta_B + \theta) + \Delta B_{13}\sin(\theta_B + \theta)\right) D_0 \cos((\omega \pm \Omega)t - (k_i \pm K_{X'})X') \\ E_3 = \left(\Delta B_{13}\cos(\theta_B + \theta) + \Delta B_{33}\sin(\theta_B + \theta)\right) D_0 \cos((\omega \pm \Omega)t - (k_i \pm K_{X'})X') \end{cases}, \quad (7)$$

where θ_B is the Bragg angle, which we put to be equal to 0.5 deg. In the case of isotropic diffraction, the frequencies of the QL AW and the shear AW are equal to $f_a \approx 200$ MHz and $f_a \approx 100$ MHz, respectively. In the case of anisotropic diffraction, the AW frequency changes

whenever the angle θ does. Then the squared EEC for the type II of AO interactions can be expressed as

$$p_{eff}^{2\,(II)} = 0.5\begin{pmatrix}(p_{11}e_1 + p_{13}e_3 + p_{15}e_5)^2\cos^2(\theta_B+\theta) + (p_{31}e_1 + p_{33}e_3)^2\sin^2(\theta_B+\theta)\\ +(p_{51}e_1 + p_{55}e_5)^2 + 0.5((p_{11}+p_{31})e_1 + (p_{13}+p_{33})e_3 + p_{15}e_5)(p_{51}e_1 + p_{55}e_5)\sin 2(\theta_B+\theta)\end{pmatrix}. \quad (8)$$

For the QT AW polarized in the *XZ* plane, the displacement components are as follows:

$$\begin{aligned} u_L &= u\cos(\pi/2+\zeta_2-\theta)\cos(\Omega t - K_{X'}X'),\\ u_T &= u\sin(\pi/2+\zeta_2-\theta)\cos(\Omega t - K_{X'}X'). \end{aligned} \quad (9)$$

Then the amplitudes of the strain components in the $X'Z'$ plane become

$$e_1' = -\sin(\zeta_2-\theta), \quad e_5' = 2e_{13}' = \cos(\zeta_2-\theta), \quad (10)$$

while in the coordinate system *XZ* they are given by

$$e_1 = -\cos\theta\sin\zeta_2, \quad e_3 = \sin\theta\cos\zeta_2, \quad e_5 = \cos(\zeta_2+\theta). \quad (11)$$

For the incident and diffracted optical waves polarized parallel to the *Y* axis, the squared EEC for the type III of AO interactions reads as

$$p_{eff}^{2\,(III)} = 0.5(p_{12}e_1 + p_{23}e_3 + p_{25}e_5)^2. \quad (12)$$

The corresponding relation valid for the incident and diffracted optical waves polarized in the *XZ* plane (i.e., for the type IV of AO interactions) is something different:

$$\begin{aligned} p_{eff}^{2\,(IV)} &= 0.5((p_{11}e_1 + p_{13}e_3 + p_{15}e_5)^2\cos^2(\theta_B+\theta) + (p_{31}e_1 + p_{33}e_3)^2\sin^2(\theta_B+\theta)\\ &+(p_{51}e_1 + p_{55}e_5)^2 + 0.5((p_{11}+p_{31})e_1 + (p_{13}+p_{33})e_3 + p_{15}e_5)(p_{51}e_1 + p_{55}e_5)\sin 2(\theta_B+\theta)) \end{aligned}. \quad (13)$$

When the PT AW is polarized parallel to the *Y* axis, the strain components caused by this AW are equal to

$$\begin{aligned} e_6 &= \cos\theta e_6',\\ e_4 &= \sin\theta e_6' \end{aligned}, \quad (14)$$

where $e_6' = \dfrac{\partial u_L}{\partial Y} + \dfrac{\partial u_T}{\partial X'} = uK_{X'}\sin(\Omega t - K_{X'}X')$ and $u_T = u\cos(\Omega t - K_{X'}X')$.

When the incident and diffracted optical waves are polarized parallel to the *Y* axis, the squared EEC for the type V of AO interactions amounts to

$$p_{eff}^{2\,(V)} = 0.5(p_{26}e_6 + p_{24}e_4)^2. \quad (15)$$

Finally, in case when the incident and diffracted optical waves are polarized in the *XZ* plane, the squared EEC for the type VI of AO interactions can be written as

$$\begin{aligned} p_{eff}^{2\,(VI)} &= 0.5((p_{16}e_6 + p_{14}e_4)^2\cos^2(\theta_B+\theta) + (p_{56}e_6 + p_{54}e_4)^2\\ &+0.5(p_{16}e_6 + p_{14}e_4)(p_{56}e_6 + p_{54}e_4)\sin 2(\theta_B+\theta)) \end{aligned}. \quad (16)$$

2.2. Anisotropic AO interactions

When the QL AW propagates in the *XZ* plane, the polarization of the incident optical wave belongs to the *XZ* plane, while the polarization of the diffracted wave is parallel to the *Y* axis. This corresponds to the type VII of AO interactions, for which the squared EEC is as follows:

$$\begin{aligned} p_{eff}^{2\,(VII)} &= E_1^2 + E_3^2 = 0.5((p_{61}e_1 + p_{65}e_5)^2\cos^2(\theta_B+\theta) + (p_{41}e_1 + p_{45}e_5)^2\sin^2(\theta_B+\theta)\\ &+(p_{61}e_1 + p_{65}e_5)(p_{41}e_1 + p_{45}e_5)\sin 2(\theta_B+\theta)) \end{aligned}. \quad (17)$$

When the QT AW is polarized in the *XZ* plane (the type VIII of AO interactions) and the polarization of optical waves is the same, the squared EEC is determined by

$$p_{eff}^{2\ (VIII)} = 0.5((p_{61}e_1 + p_{65}e_5)^2 \cos^2(\theta_B + \theta) + (p_{41}e_1 + p_{45}e_5)^2 \sin^2(\theta_B + \theta) + (p_{61}e_1 + p_{65}e_5)(p_{41}e_1 + p_{45}e_5)\sin 2(\theta_B + \theta)) \quad (18)$$

Finally, the squared EEC for the case of PT AW polarized parallel to the *Y* axis and the same polarizations of the optical waves (i.e., the type IX of AO interactions) is given by

$$p_{eff}^{2\ (IX)} = 0.5((p_{66}e_6 + p_{64}e_4)^2 \cos^2(\theta_B + \theta) + (p_{46}e_6 + p_{44}e_4)^2 \sin^2(\theta_B + \theta) + (p_{66}e_6 + p_{64}e_4)(p_{46}e_6 + p_{44}e_4)\sin 2(\theta_B + \theta)). \quad (19)$$

2.3. Numerical method

Solving the Christoffel equation $M_{kl}u_l^0 = \rho v^2 u_k^0$ (e.g., for the crystallographic plane *ac*), one can obtain the eigenvectors u_l^0, u_k^0 for the QL AWs,

$$\begin{cases} (M_{11} - \lambda_{11}(\theta))u_1^0 + M_{13}u_3^0 = 0 \\ (M_{22} - \lambda_{11}(\theta))u_2^0 = 0 \\ M_{13}u_1^0 + (M_{33} - \lambda_{11}(\theta))u_3^0 = 0 \end{cases}, \quad (20)$$

and the eigenvectors for the QT AWs,

$$\begin{cases} (M_{11} - \lambda_{33}(\theta))u_1^0 + M_{13}u_3^0 = 0 \\ (M_{22} - \lambda_{33}(\theta))u_2^0 = 0 \\ M_{13}u_1^0 + (M_{33} - \lambda_{33}(\theta))u_3^0 = 0 \end{cases}. \quad (21)$$

Here

$$\lambda_{11,33}(\theta) = \frac{M_{11}(\theta) + M_{33}(\theta)}{2} \pm \frac{\sqrt{(M_{11}(\theta) - M_{33}(\theta))^2 + 4M_{13}(\theta)^2}}{2}, \quad \lambda_{22}(\theta) = M_{22}(\theta), \quad (22)$$

are eigenvalues of the Christoffel tensor for the *ac* plane [8].

The eigenvectors for the QL and QT AWs have the form

$$\begin{pmatrix} u_1^0(\theta) \\ 0 \\ u_3^0(\theta) \end{pmatrix}. \quad (23)$$

Thus, the displacement components can be written as

$$\begin{aligned} \boldsymbol{u}_1 &= \boldsymbol{u}_1^0(\theta)\cos(\Omega t - (\boldsymbol{k}_1 X + \boldsymbol{k}_3 Z)), \\ \boldsymbol{u}_3 &= \boldsymbol{u}_3^0(\theta)\cos(\Omega t - (\boldsymbol{k}_1 X + \boldsymbol{k}_3 Z)). \end{aligned} \quad (24)$$

Then the components of the strain tensor are as follows:

$$\begin{aligned} e_1 &= \frac{\partial u_1}{\partial X} = u_1^0(\theta)K_1 \sin(\Omega t - (K_1 X + K_3 Z)) = u_1^0(\theta)K\cos\theta\sin(\Omega t - (K_1 X + K_3 Z)), \\ e_3 &= \frac{\partial u_3}{\partial Z} = u_3^0(\theta)K_3 \sin(\Omega t - (K_1 X + K_3 Z)) = u_3^0(\theta)K\sin\theta\sin(\Omega t - (K_1 X + K_3 Z)), \\ e_5 &= 2e_{13} = \frac{\partial u_1}{\partial Z} + \frac{\partial u_3}{\partial X} = (u_1^0(\theta)K_3 + u_3^0(\theta)K_1)\sin(\Omega t - (K_1 X + K_3 Z)) \\ &= K(u_1^0(\theta)\sin\theta + u_3^0(\theta)\cos\theta)\sin(\Omega t - (K_1 X + K_3 Z)). \end{aligned} \quad (25)$$

For the QL AW we have

$$u_1^0(\theta) = -\frac{0.5(C_{13}+C_{55})\sin 2\theta + C_{15}\cos^2\theta}{\sqrt{(C_{11}\cos^2\theta + C_{55}\sin^2\theta + C_{15}\sin 2\theta - \lambda_{11}(\theta))^2 + (0.5(C_{13}+C_{55})\sin 2\theta + C_{15}\cos^2\theta)^2}}, \quad (26)$$

$$u_3^0(\theta) = \frac{C_{11}\cos^2\theta + C_{55}\sin^2\theta + C_{15}\sin 2\theta - \lambda_{11}(\theta)}{\sqrt{(C_{11}\cos^2\theta + C_{55}\sin^2\theta + C_{15}\sin 2\theta - \lambda_{11}(\theta))^2 + (0.5(C_{13}+C_{55})\sin 2\theta + C_{15}\cos^2\theta)^2}}, \quad (27)$$

where

$$\lambda_{11}(\theta) = \sqrt{\frac{M_{11}(\theta)+M_{33}(\theta)+\sqrt{(M_{11}(\theta)-M_{33}(\theta))^2+4M_{13}^2(\theta)}}{2\rho}}$$

$$= \sqrt{\frac{(C_{11}+C_{55})\cos^2\theta + (C_{55}+C_{33})\sin^2\theta + C_{15}\sin 2\theta}{2\rho} + \frac{\sqrt{((C_{11}-C_{55})\cos^2\theta + (C_{55}-C_{33})\sin^2\theta + C_{15}\sin 2\theta)^2 + 4(0.5(C_{13}+C_{55})\sin 2\theta + C_{15}\cos^2\theta)^2}}{2\rho}}. \quad (28)$$

For the QT AW we have

$$u_1^0(\theta) = \frac{0.5(C_{13}+C_{55})\sin 2\theta + C_{15}\cos^2\theta}{\sqrt{(C_{11}\cos^2\theta + C_{55}\sin^2\theta + C_{15}\sin 2\theta - \lambda_{33}(\theta))^2 + (0.5(C_{13}+C_{55})\sin 2\theta + C_{15}\cos^2\theta)^2}}, \quad (29)$$

$$u_3^0(\theta) = \frac{C_{55}\sin^2\theta - C_{11}\cos^2\theta + C_{15}\sin 2\theta + \lambda_{33}(\theta)}{\sqrt{(C_{11}\cos^2\theta + C_{55}\sin^2\theta + C_{15}\sin 2\theta - \lambda_{33}(\theta))^2 + (0.5(C_{13}+C_{55})\sin 2\theta + C_{15}\cos^2\theta)^2}}, \quad (30)$$

where

$$\lambda_{33}(\theta) = \sqrt{\frac{M_{11}(\theta)+M_{33}(\theta)-\sqrt{(M_{11}(\theta)-M_{33}(\theta))^2+4M_{13}^2(\theta)}}{2\rho}}$$

$$= \sqrt{\frac{(C_{11}+C_{55})\cos^2\theta + (C_{55}+C_{33})\sin^2\theta + C_{15}\sin 2\theta}{2\rho} - \frac{\sqrt{((C_{11}-C_{55})\cos^2\theta + (C_{55}-C_{33})\sin^2\theta + C_{15}\sin 2\theta)^2 + 4(0.5(C_{13}+C_{55})\sin 2\theta + C_{15}\cos^2\theta)^2}}{2\rho}}. \quad (31)$$

As expected (see Fig. 2), the dependences of the strain tensor components on the angle θ calculated using Eq. (3) and Eqs. (27) – (33) prove to be the same.

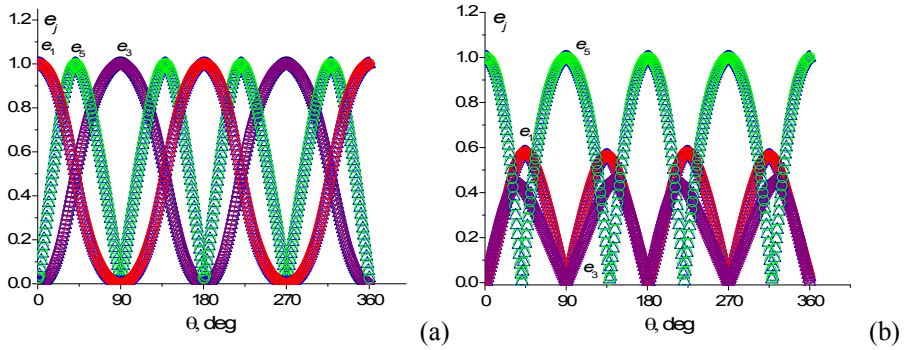

Fig. 2. Dependences of strain tensor components caused by the QL (a) and QT (b) AWs. Triangles and circles correspond to calculations performed using analytical and numerical approaches, respectively.

3. Results and discussion

The dependence of the cube of AW slowness on the angle θ has been obtained following from the Christoffel equation and using the elastic stiffnesses taken from Ref. [14]: $C_{11} = 68.4\times10^9$ N/m^2, $C_{12} = 26.8\times10^9$ N/m^2, $C_{13} = 17.9\times10^9$ N/m^2, $C_{33} = 94.3\times10^9$ N/m^2, $C_{14} = 0.0$, $C_{25} = 1.2\times10^9$ N/m^2, $C_{44} = 22.6$ and $C_{66} = 20.8\times10^9$ N/m^2. The EECs have been calculated using the elasto-optic coefficients determined by us: $p_{12} = 0.177\pm0.005$, $p_{13} = 0.119\pm0.006$, $p_{31} = 0.136\pm0.016$, $p_{14} = 0.005\pm0.006$, $p_{15} = 0.011\pm0.002$, $p_{16} = -0.008\pm0.001$, $p_{41} = 0.005\pm0.013$, $p_{51} = -0.002\pm0.013$, $p_{44} = -0.025\pm0.012$ and $p_{45} = -0.003\pm0.014$ [15], and $p_{11} = 0.162\pm0.009$ and $p_{33} = 0.159\pm0.009$ [6]. The refractive indices for the linearly polarized optical eigenwaves amount to $n_e = 2.151$ and $n_o = 2.116$ at the light wavelength $\lambda = 632.8$ nm [1].

Fig. 3 shows dependences of the squared EEC and the AO figure of merit on the angle θ for the types I and II of isotropic AO interactions with the QL AW in $Pb_5Ge_3O_{11}$. The angular dependences of the EEC and the AO figure of merit are almost the same under conditions when the non-orthogonality of AWs is accounted for or neglected.

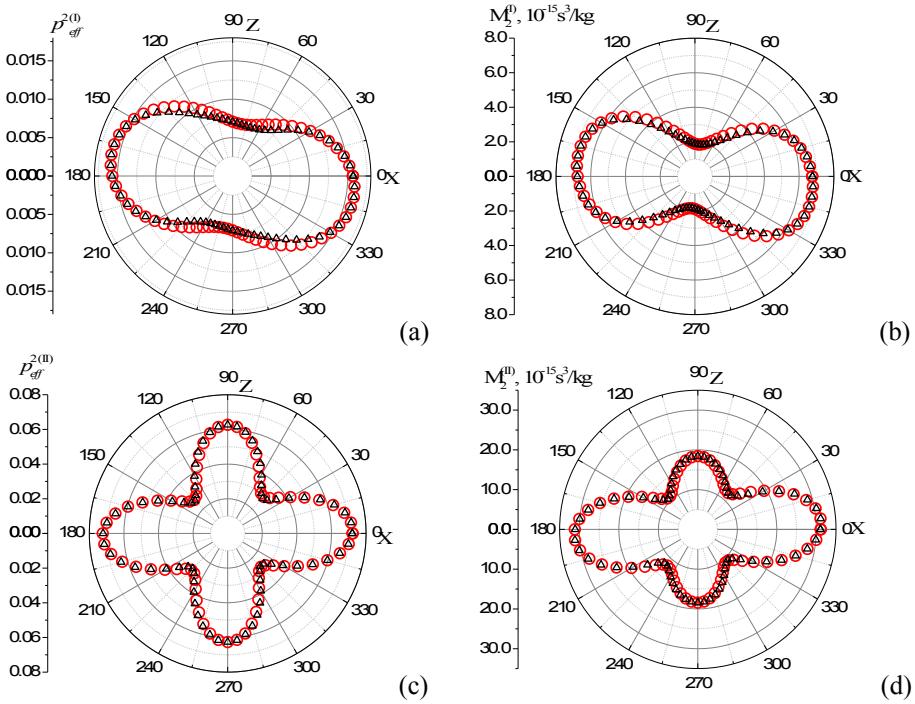

Fig. 3. Dependences of squared EEC (a, c) and AO figure of merit (b, d) on the angle θ for the types I (a, b) and II (c, d) of isotropic AO interactions with the QL AW in $Pb_5Ge_3O_{11}$. Open triangles correspond to the data calculated with accounting for the non-orthogonality of AWs and open circles correspond to its neglect.

The maximal AO figure of merit (31.3×10^{-15} s^3/kg) is achieved at the AO interactions of the type II, when the angles are equal to $\theta = 3.0$ and 183.0 deg (Fig. 3d). However, when the AW propagates almost parallel to the X axis, the incident and diffracted optical waves propagate at the angle ±0.5 deg with respect to the Z axis. Notice that the lead germanate crystals have the optical activity (±5.58 deg/mm, with the corresponding gyration component being equal to $g_{33} = \pm4.16\times10^{-5}$ at $\lambda = 632.8$ nm [1]). The module of the gyration component g_{11} has been found to be equal to 10.5×10^{-5} at $\lambda = 632.8$ nm [16], whereas its sign is the same as for the g_{33}

component. When the optical waves propagate along the directions almost parallel to the optic axis, the eigenwaves are nearly circularly polarized.

As shown in our recent work [6], the AO figure of merit for the case of isotropic diffraction of circularly polarized optical waves at the QL AW propagating along the *X* axis is equal to 12.4×10^{-15} s^3/kg, which is almost three times smaller than the value obtained in the present work for the interaction of linearly polarized optical waves. The reason for this disagreement is caused by the fact that we neglect the effect of optical activity on the polarization of optical eigenwaves.

Let us determine the angle of propagation of the incident and diffracted optical waves at which one can neglect the ellipticity of optical eigenwaves and the effect introduced by the optical activity. The ellipticity of the optical eigenwaves is determined by the formula [17]

$$\kappa(\varphi)=\frac{1}{2G(\varphi)}\left((n_e^2(\varphi)-n_o^2)-\sqrt{(n_e^2(\varphi)-n_o^2)^2+4G^2(\varphi)}\right), \tag{32}$$

where the scalar gyration parameter is equal to $G(\varphi)=g_{33}\cos^2\varphi+g_{11}\sin^2\varphi$, the refractive index is given by $n_e^2(\varphi)=\dfrac{n_o^2n_e^2}{n_e^2\sin^2\varphi+n_o^2\cos^2\varphi}$, and φ denotes the angle between the *Z* axis and the propagation direction of the optical wave.

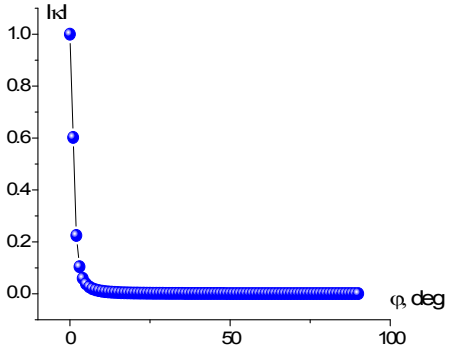

Fig. 4. Dependence of ellipticity modulus $|\kappa|$ for the optical eigenwaves on the angle of light propagation with respect to the *Z* axis.

The dependence of the ellipticity of optical eigenwaves on the propagation angle is presented in Fig. 4. Let us accept that a reduction of ellipticity by the two orders of magnitude from the value peculiar for the pure circularly polarized waves $\kappa=\pm1$ (i.e., down to the ellipticity value ±0.01) is enough for neglecting the effect of optical activity. The AO figure of merit for the type II of AO interactions is equal to 31.3×10^{-15} s^3/kg when the incident and diffracted optical waves propagate at the angle (3.0±0.5) deg relative to the *Z* axis. At the angle 10 deg with respect to the *Z* axis, the ellipticity decreases by the two orders of magnitude, i.e. to 0.01. Under this condition, the AO figure of merit changes its value only slightly (30.3×10^{-15} s^3/kg).

For the type I of AO interactions, the maximal AO figure of merit, 6.8×10^{-15} s^3/kg, is reached at the angles θ equal to 351 or 171 deg (see Fig. 3b).

The dependences of EEC and AO figure of merit for the types III and IV of AO interactions with the QT AW are shown in Fig. 5. The influence of non-orthogonality of the AW QT on the EEC and the AO figure of merit at the type IV of interactions is not essential (see Fig. 5c, d), although the non-orthogonality affects notably these parameters at the AO interactions of the type III (see Fig. 5a, b). As a result, the maximal AO figure of merit (2.4×10^{-15} s^3/kg) reached at the angles $\theta=122$ and 302 deg is essentially higher than the corresponding maximal value (0.76×10^{-15} s^3/kg) achieved under alternative condition when the non-orthogonality of AW polarizations is neglected. Besides, the angular positions of the maximums are shifted by 3 deg.

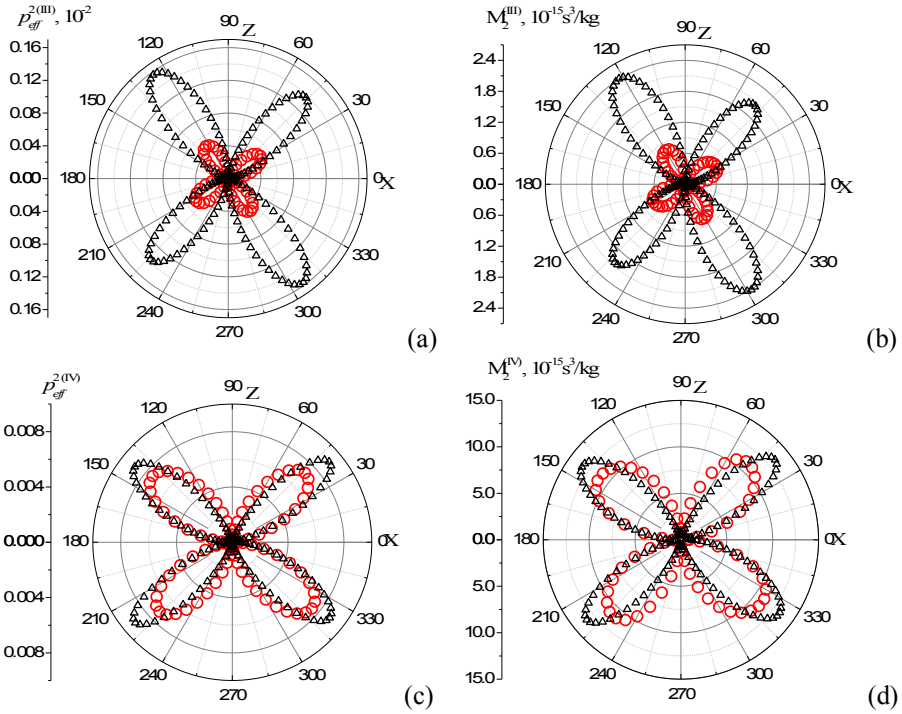

Fig. 5. Dependences of squared EEC (a, c) and AO figure of merit (b, d) on the angle θ for the types III (a, b) and IV (c, d) of isotropic AO interactions with the QT AW in $Pb_5Ge_3O_{11}$. Open triangles correspond to the data calculated with accounting for the non-orthogonality of AWs and open circles correspond to its neglect.

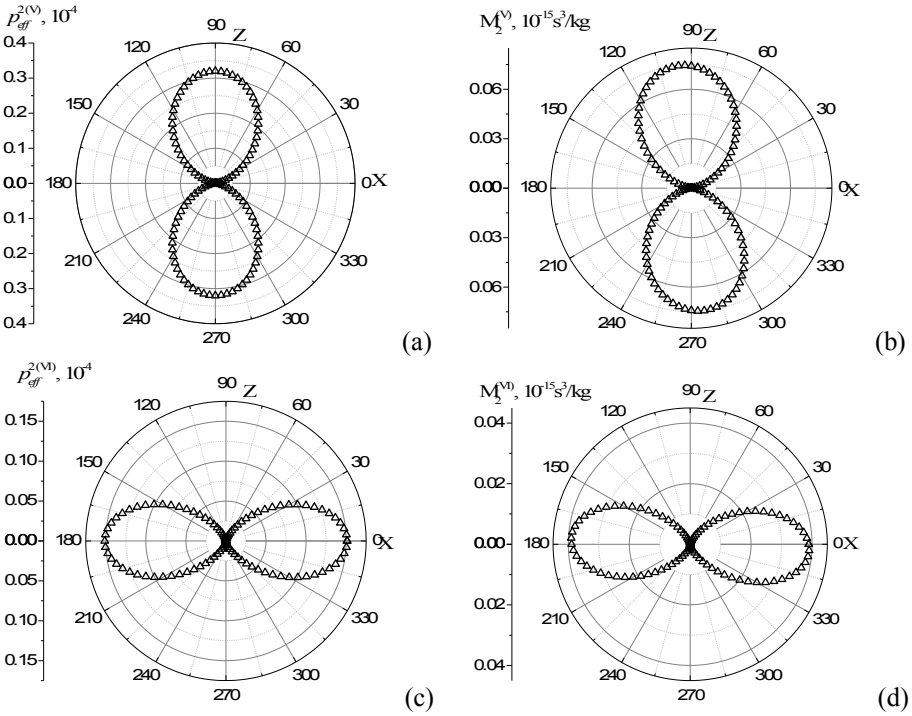

Fig. 6. Dependences of squared EEC (a, c) and AO figure of merit (b, d) on the angle θ for the types V (a, b) and VI (c, d) of isotropic AO interactions with the PT AW in $Pb_5Ge_3O_{11}$.

For the types V and VI of AO interactions with the PT AW, the EEC and the AO figure of merit (see Fig. 6) are the same, irrespective of whether we consider or neglect the non-ortogonality of AW polarizations. The AO figure of merit at these interaction types is very small and does not exceed ~ 4×10^{-17} s^3/kg and ~ 7×10^{-17} s^3/kg respectively for the types VI and V of AO interactions.

The same is true concerning the types VII and VIII of anisotropic AO interactions. The AO figure of merit remains small enough and does not to exceed $10^{-17} \div 10^{-18}$ s^3/kg (see Fig. 7 and Fig. 8). The differences of the EECs and the AO figures of merit observed under conditions when the non-orthogonality of AWs is considered or neglected are not significant.

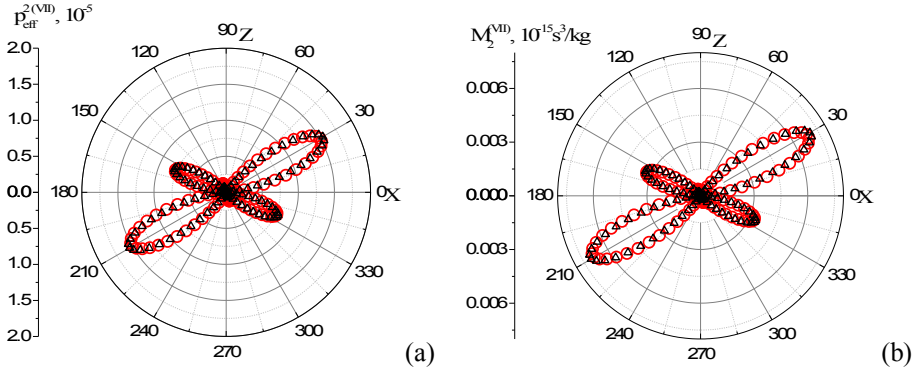

Fig. 7. Dependences of squared EEC (a) and AO figure of merit (b) on the angle θ for the type VII of anisotropic AO interactions with the QL AW in $Pb_5Ge_3O_{11}$. Open triangles correspond to the data calculated with accounting for the non-orthogonality of AWs and open circles correspond to its neglect.

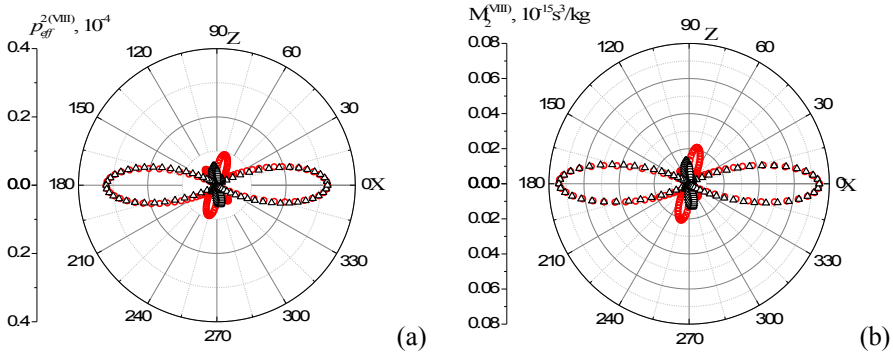

Fig. 8. Dependences of squared EEC (a) and AO figure of merit (b) on the angle θ for the type VIII of anisotropic AO interactions with the QT AW in $Pb_5Ge_3O_{11}$. Open triangles correspond to the data calculated with accounting for the non-orthogonality of AWs and open circles correspond to its neglect.

In case of the type IX of AO interactions (see Fig. 9) with the PT AW and anisotropic type of diffraction, the AO figure of merit reaches a rather high value at $\theta = 0$ and 180 deg, 13.3×10^{-15} s^3/kg. When calculating the propagation direction for the incident and diffracted optical waves, one can use a formula from Ref. [18] (see Fig. 10a) modified to the case of our phase-matching conditions (Fig. 10b):

$$\theta = 180 - \mathrm{a\,tan}\left(\frac{n_o n_e \dfrac{\sin\varphi_i}{\sqrt{n_o^2\cos^2\varphi_i + n_e^2\sin^2\varphi_i}} - n_o\sin(\varphi_i+\gamma)}{n_o n_e \dfrac{\cos\varphi_i}{\sqrt{n_o^2\cos^2\varphi_i + n_e^2\sin^2\varphi_i}} - n_o\cos(\varphi_i+\gamma)} \right). \tag{33}$$

Here φ_i is the angle between the X axis and the propagation direction of the incident optical wave and γ the diffraction angle, which is equal to 1 deg in our case.

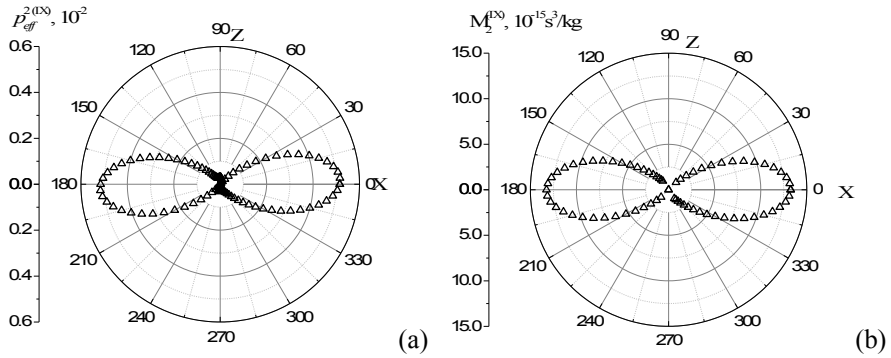

Fig. 9. Dependences of squared EEC (a) and AO figure of merit (b) on the angle θ for the type IX of anisotropic AO interactions with the PT AW in $Pb_5Ge_3O_{11}$.

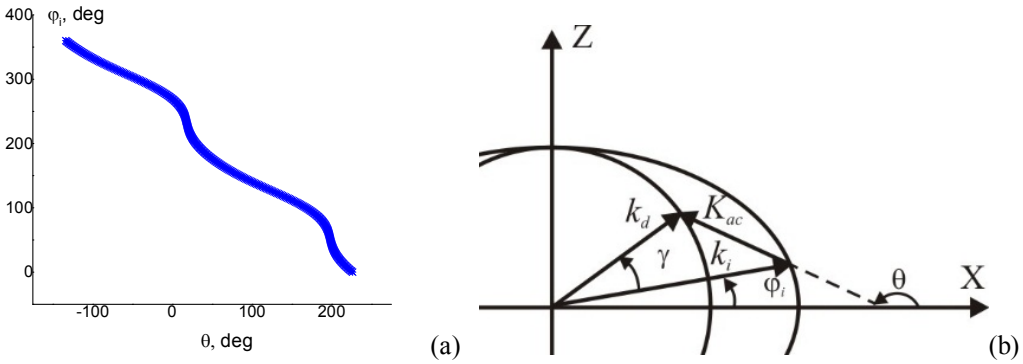

Fig. 10. Dependence of angle between the propagation direction of incident optical wave and the X axis on the angle θ (a), and a schematic view of phase-matching conditions (b).

The dependence of the angle φ_i on the angle θ is nonlinear. When the AW propagates along the X axis (i.e., we have $\theta = 0$ or 180 deg), the incident optical wave propagates at the angles $\varphi_i = 269.5$ deg or 89.5 deg, which is almost parallel to the optic axis. Under these conditions, the ellipticity of the optical eigenwaves is close to unity. When $\varphi_i = 80$ deg (i.e., when the ellipticity of the incident optical eigenwaves decreases to 0.01), the angle θ acquires the value –187.9 deg. At this angle of incidence of the optical wave, the AO figure of merit decreases insignificantly and becomes equal to 12.4×10^{-15} s^3/kg.

4. Conclusion

In the present work, we have found agreement between the data of numerical and analytical approaches used for computing the anisotropy of the EEC and the AO figure of merit. The appropriate studies have been carried out on the example of AO interactions occurring in the XZ plane of $Pb_5Ge_3O_{11}$. The anisotropy of AO figure of merit in this crystal has been studied for the first time. We have demonstrated that, in the approximation of linearly polarized optical eigenwaves, the most reliable maximal value of the AO figure of merit for the case of isotropic diffraction is equal to 30.3×10^{-15} s^3/kg. It is achieved at the AO interactions of the type II. For the anisotropic diffraction, the maximal AO figure of merit, 12.4×10^{-15} s^3/kg, is reached at the AO interactions of the type IX and the angle θ equal to 187.9 deg.

Acknowledgement

The authors acknowledge the Ministry of Education and Science of Ukraine for financial support of the present study (the Projects # 0120U102031 and #0121U109804).

References

1. Iwasaki H, Miyazawa S, Koizumi H, Sugii K and Niizeki N, 1972. Ferroelectric and optical properties of $Pb_5Ge_3O_{11}$ and its isomorphous compound $Pb_5Ge_2SiO_{11}$. J. Appl. Phys. **43**: 4907–4915.
2. Shaskolskaya M P. Acoustic crystals. Moscow: Nauka (1982).
3. Dougherty J P, Sawaguchi E and Cross L E, 1972. Ferroelectric optical rotation domains in single crystal $Pb_5Ge_3O_{11}$. Appl. Phys. Lett. **20**: 364–365.
4. Mys Oksana, Martynyuk-Lototska Iryna, Pogodin Artem, Dudok Taras, Adamenko Dmitro, Krupych Oleh, Skab Ihor, and Vlokh Rostyslav, 2019. Acousto-optic interaction between circularly polarized optical eigenwaves: example of $AgGaS_2$ crystals. Appl. Opt. **58**: 6012-6018.
5. Mys O, Adamenko D, Skab I and Vlokh R, 2019. Anisotropy of acousto-optic figure of merit for the collinear diffraction of circularly polarized optical waves at the wavelength of isotropic point in $AgGaS_2$ crystals. Ukr. J. Phys. Opt. **20**: 73–80.
6. Mys O, Krupych O, Martynyuk-lototska I, Orykhivskyi I, Kostyrko M and Vlokh R. 2021. Types of acousto-optic interactions between acoustic and circularly polarized optical waves. Case of $Pb_5Ge_3O_{11}$ crystals. Appl. Opt. **60**: 2846–2853.
7. Iwasaki H and Sugii K, 1971. Optical activity of ferroelectric $5PbO_3{\cdot}GeO_2$ single crystals. Appl. Phys. Lett. **19**: 92–93.
8. Sirotin YuI and Shaskolskaya M P. Fundamentals of crystal physics. Moscow: Mir Publishers (1982).
9. Martynyuk-lototska I, Mys O, Dudok T, Mytsyk B, Demyanyshyn N, Kostyrko M, Adamenko D, Trubitsyn M and Vlokh R. 2020. Experimental determination of full matrices of the piezo-optic and elasto-optic coefficients for $Pb_5Ge_3O_{11}$ crystals. Appl. Opt. **59**: 6717–6723.
10. Brugger K, 1965. Pure modes for elastic waves in crystals. J. Appl. Phys. **36**: 759–768.
11. Fedorov F I. Theory of elastic waves in crystals. Springer Science & Business Media (1968).
12. Mys O, Adamenko D, Kostyrko M and Vlokh R, 2019. Conditions for analytical description of anisotropy of acousto-optic figure of merit under consideration of polarization non-orthogonality of acoustic waves. Ukr. J. Phys. Opt. **20**: 175–185.
13. Mys O, Adamenko D, Krupych O and Vlokh R, 2018. Effect of deviation from purely transverse and longitudinal polarization states of acoustic waves on the anisotropy of acousto-optic figure of merit: the case of Tl_3AsS_4 crystals. Appl. Opt. **57**: 8320–8330.
14. Yamada T, Iwasaki H and Niizeki N, 1972. Elastic and piezoelectric properties of ferroelectric $5PbO_3{\cdot}GeO_2$ crystals. J. Appl. Phys. **43**: 771–775.
15. Martynyuk-Lototska I, Mys O, Dudok T, Mytsyk B, Demyanyshyn N, Kostyrko M, Adamenko D, Trubitsyn M and Vlokh R, 2020. Experimental determination of full matrices of the piezo-optic and elasto-optic coefficients for $Pb_5Ge_3O_{11}$ crystals. Appl. Opt. **59**: 6717–6723.
16. Vlokh O, Kushnir O and Shopa Ya, 1992. Gyrotropic properties of $Pb_5Ge_3O_{11}$ ferroelectric crystals. Ferroelectrics. **126**: 97–102.
17. Konstantinova A F, Grechushnikov B N, Bokut B V and Valyashko E G. Optical properties of crystals. Minsk: Navuka i Technika (1995).
18. Mys O, Kostyrko M and Vlokh R, 2016. Anisotropy of acousto-optic figure of merit for LiNbO3 crystals: anisotropic diffraction. Appl. Opt. 55: 2439–2450.

Mys O., Orykhivskyi I., Kostyrko M. and Vlokh R. 2021. Anisotropy of acousto-optic figure of merit in the *XZ* plane of $Pb_5Ge_3O_{11}$ crystals. Ukr.J.Phys.Opt. **22**: 110 – 122.
doi: 10.3116/16091833/22/2/110/2021

Анотація. *Використано числовий і аналітичний підходи до виведення феноменологічних співвідношень для ефективних еластооптичних коефіцієнтів (ЕЕК). Анізотропію ЕЕК і показника акустооптичної (АО) якості розраховано для конкретного випадку АО-взаємодій у головній площині XZ кристалів $Pb_5Ge_3O_{11}$. Використовуючи наближення лінійно поляризованих оптичних власних хвиль, нами знайдено, що максимальний показник АО-якості для ізотропної дифракції дорівнює $30,3\times10^{-15}$ $с^3/кг$. Він досягається для випадку АО-взаємодій типу II під кутом $\theta = 10$ град відносно осі X. У разі анізотропної АО-дифракції відповідний максимум $12,4\times10^{-15}$ $с^3/кг$ має місце для АО-взаємодій типу IX під кутом $\theta = 187,9$ град.*